

TABLE XII

CHEMICAL COMPOSITION OF ZEOLITE FCC CATALYSTS

Catalyst ID	Nominal Composition	Comment
9669-152	40% LZY-84 zeolite 20.8% Ludox AS-40 (silica sol) 4.2% Catapal alumina 35% Kaolin clay	Standard Y
9669-153	34.7% Ludox AS-40 (silica sol) 7% Catapal alumina 58.3% Kaolin clay	Matrix only
9669-154	10% LZY-84 20.8% Ludox AS-40 (silica sol) 4.2% Catapal alumina 65% Kaolin clay	Low Y zeolite
9669-155	10% Beta 20.8% Ludox AS-40 (silica sol) 4.2% Catapal alumina 65% Kaolin clay	Low Beta

techniques. The actual zeolite concentrations in the finished catalysts were not measured. The BET surface areas of these catalysts, after a steam treatment of 1450°F for 5 hours, are found in Table XIII. The surface areas and pore volumes decreased with the lower zeolite levels, as expected.

Runs were made with these catalysts using a catalyst to oil ratio of 0.75 and reaction temperatures of 970°F and 880°F. The conversions reported were calculated from the 430-°F fraction of the GC simulated distillation of the total liquid products. Figure 42 shows that the "SD" method gives a conversion value that is in reasonable agreement with conversion value that is obtained by the normal "MYU" method, which is the sum of product C- gas, gasoline and coke. The "SD" method also allowed calculation of the yields of light cycle oil (430-650°F) and heavy cycle oil (650+°F) products.

Figures 43-49 show that the yields of propylene, isobutylene, isoamylenes, gasoline, 430-650, 650-800, and 800+°F products, respectively, all increased with increasing conversion. No clear trends were seen that would distinguish between these catalysts.

4.2 LaPorte Wax Feedstock

Wax produced by the slurry phase Fischer-Tropsch process at the LaPorte plant currently contains over 2% catalyst contaminants, as Table II shows. That level of contamination is too high for it to be converted into transportation fuels using any fixed-bed process. However, it might be upgradable by the FCC process, which operates with a circulating catalyst inventory, if the F-T catalyst could be selectively removed from the FCC unit. These F-T fines will deposit on the external surfaces of the FCC catalyst microspheres. One possible removal method is to selectively attrit the F-T catalyst from the external surfaces of the FCC catalyst.

FIGURE 42

SASOL WAX MYU DATA: PARITY PLOT
OF MYU AND SIMULATED DISTILLATION METHODS
FOR CONVERSION CALCULATION

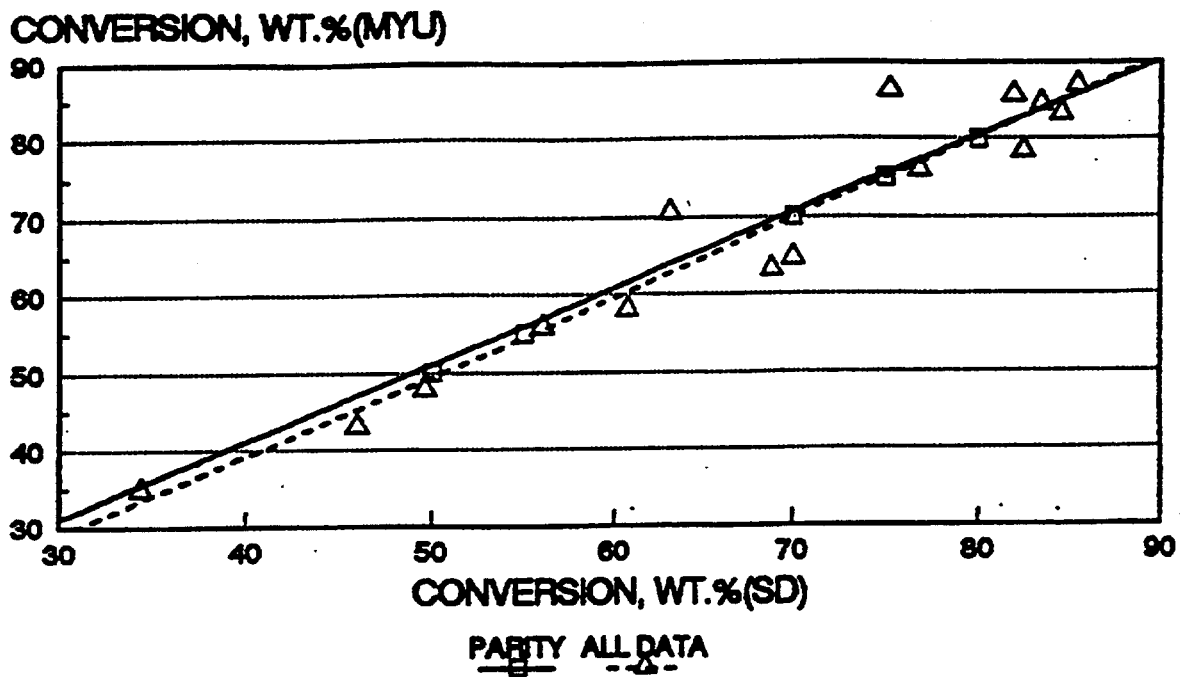
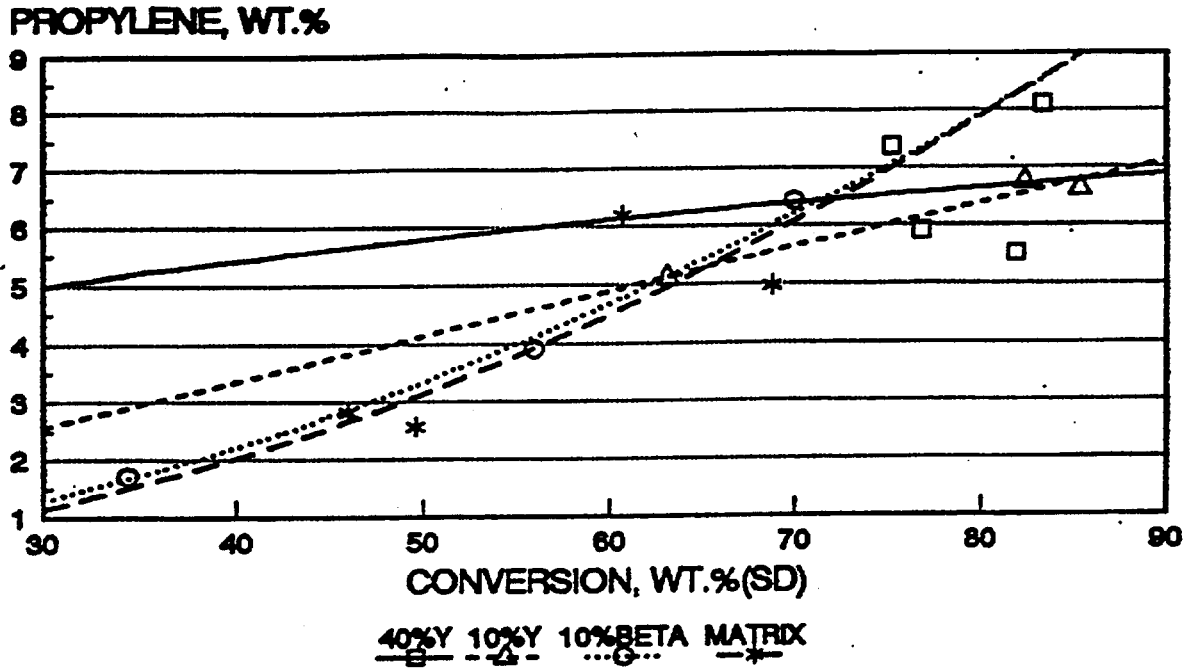


FIGURE 43

SASOL WAX MYU DATA: EFFECT OF CONVERSION ON PROPYLENE YIELD
WITH LOW ZEOLITE CONTENT CATALYSTS

a. Distinguishing Catalysts



b. Not Distinguishing Catalysts

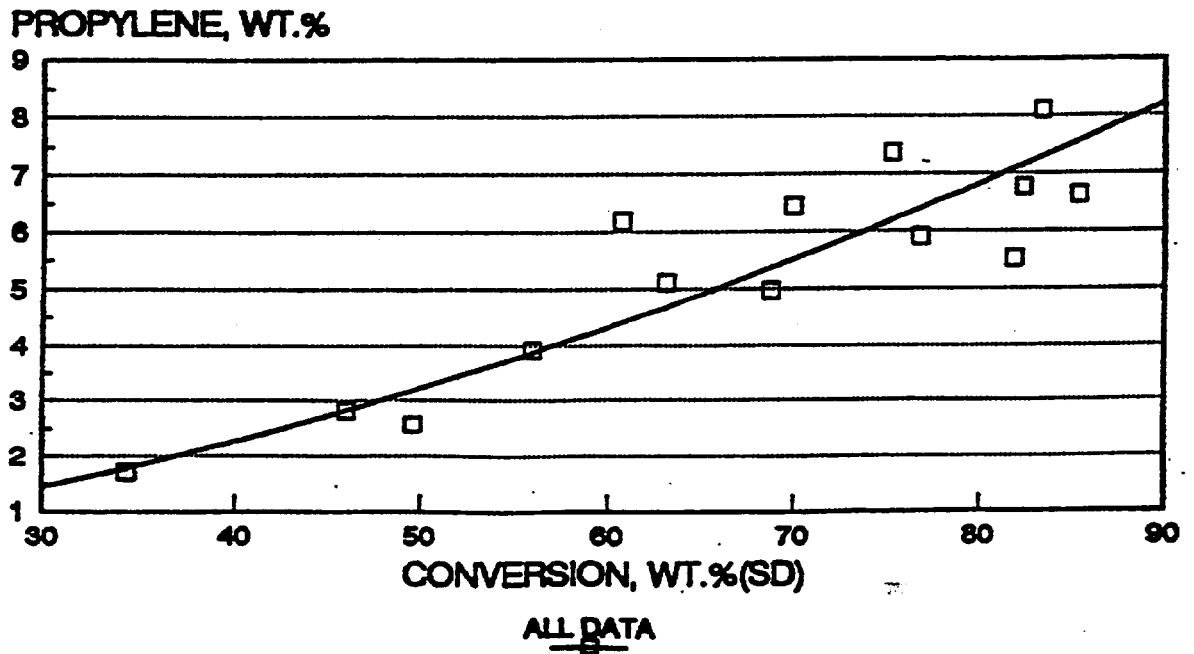
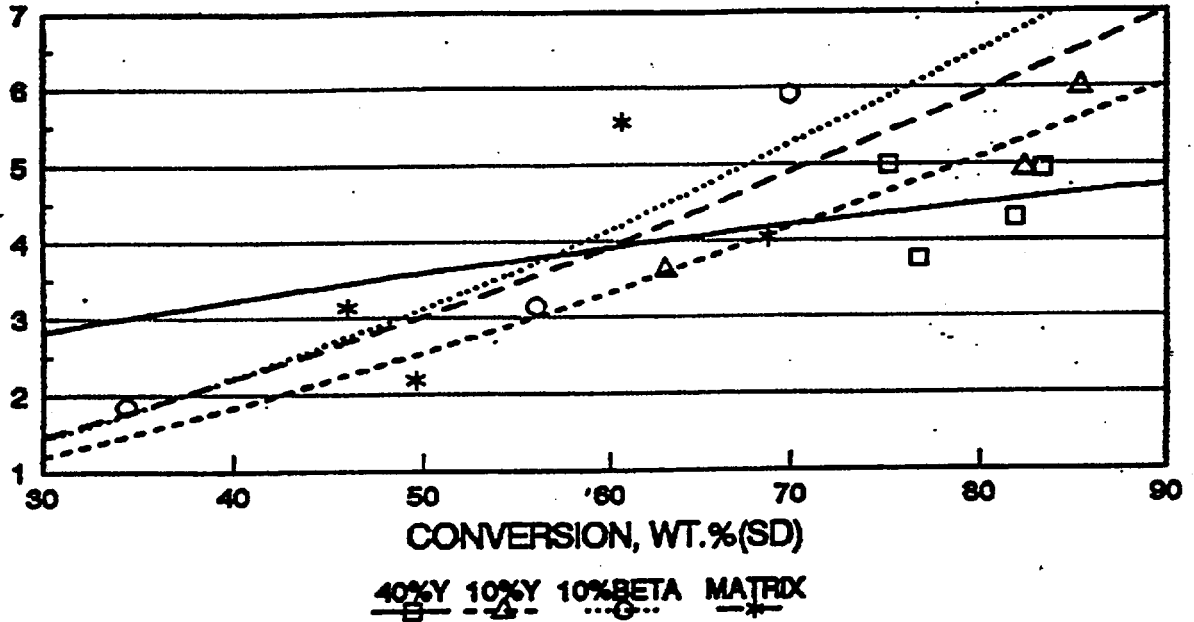


FIGURE 44

SASOL WAX MYU DATA: EFFECT OF CONVERSION ON ISOBUTYLENE YIELD
WITH LOW ZEOLITE CONTENT CATALYSTS

a. Distinguishing Catalysts

ISOBUTYLENE, WT.%



b. Not Distinguishing Catalysts

ISOBUTYLENE, WT.%

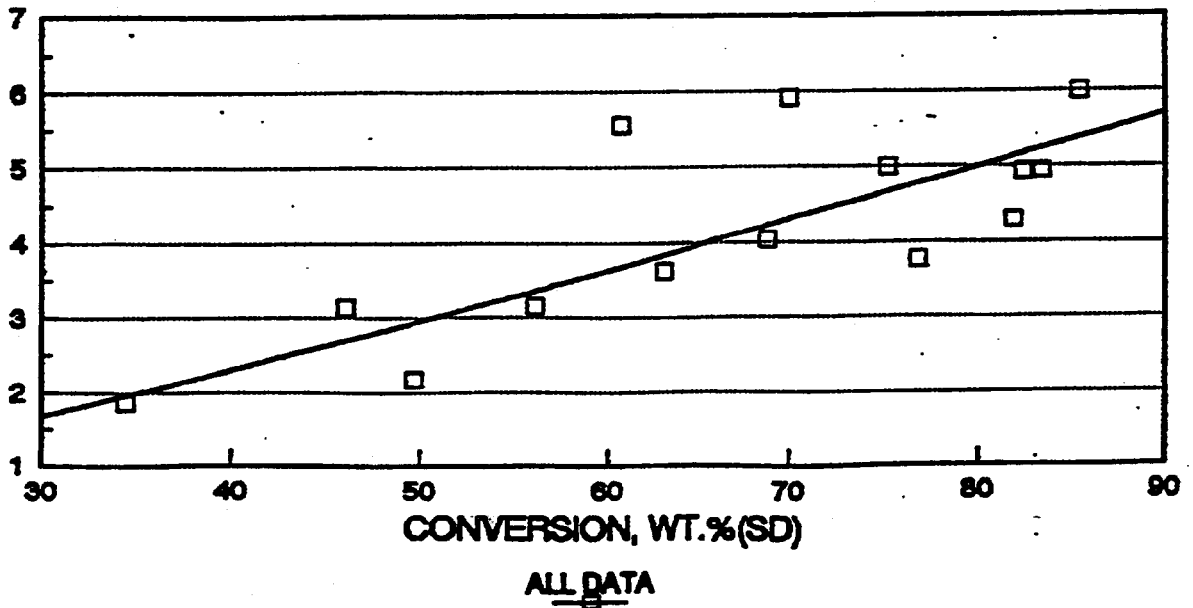
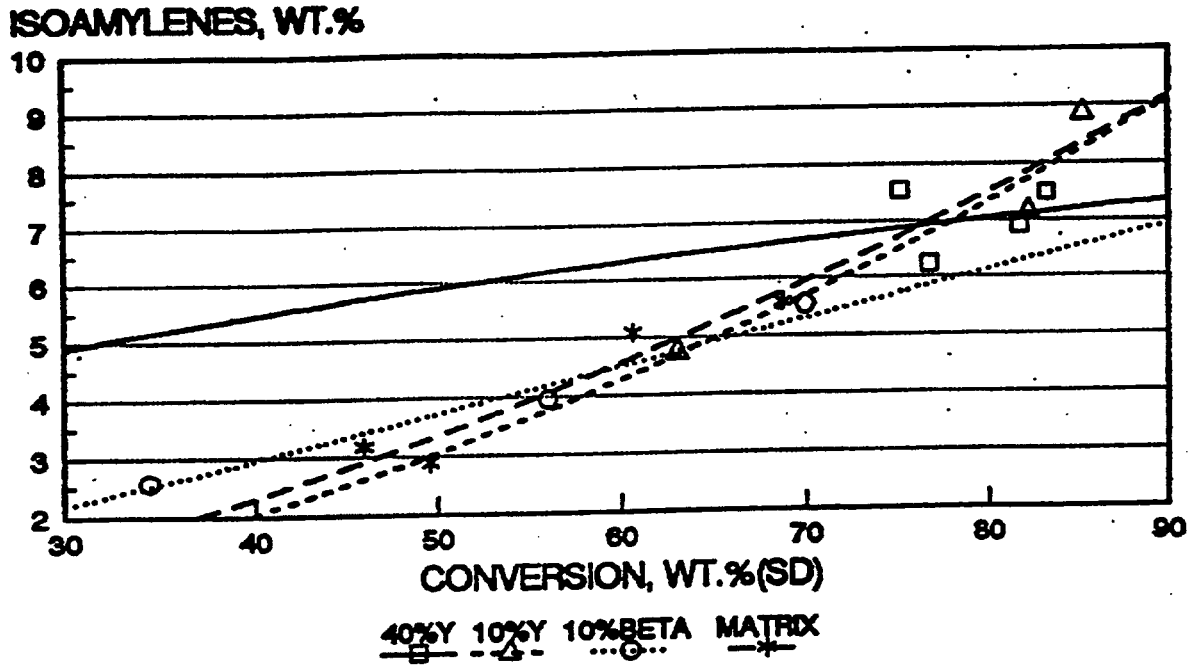


FIGURE 45

SASOL WAX MYU DATA: EFFECT OF CONVERSION ON ISOAMYLENES YIELD WITH LOW ZEOLITE CONTENT CATALYSTS

a. Distinguishing Catalysts



b. Not Distinguishing Catalysts

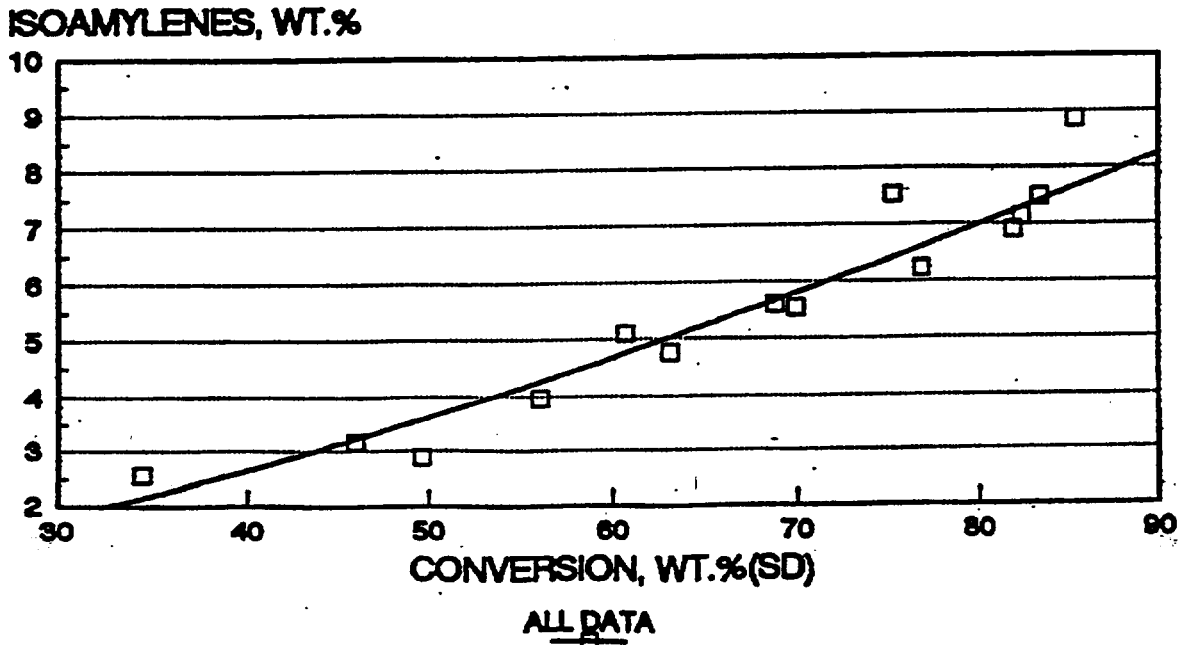


FIGURE 46

SASOL WAX MYU DATA: EFFECT OF CONVERSION
ON C5-430f NAPHTHA YIELD
WITH LOW ZEOLITE CONTENT CATALYSTS

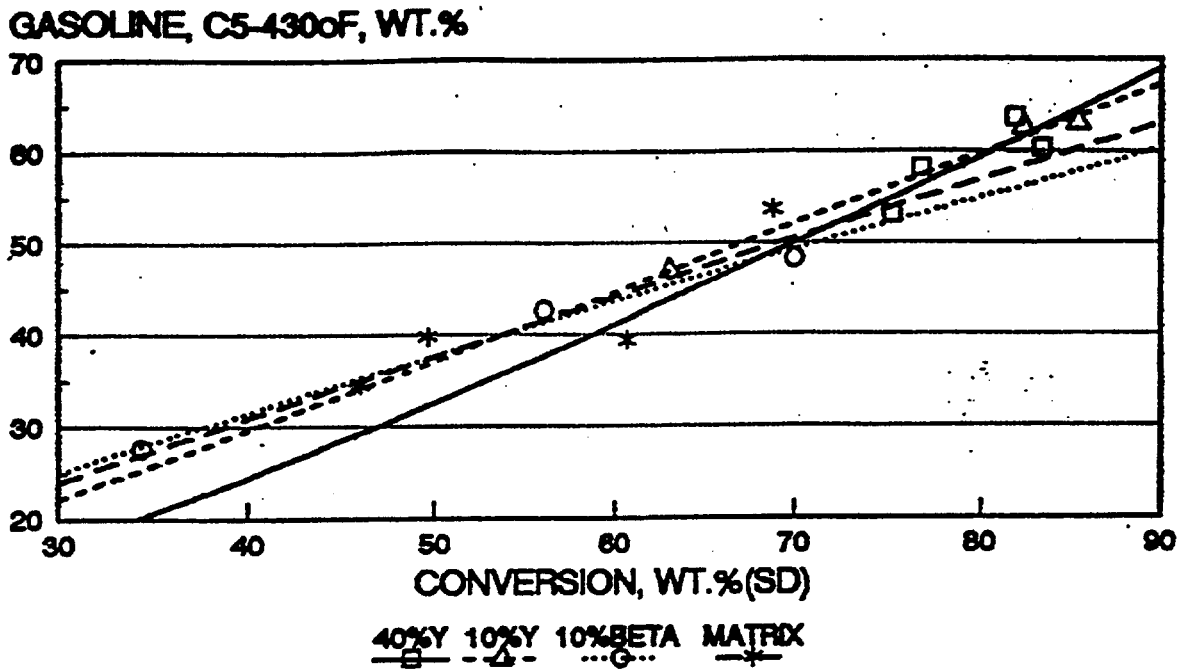


FIGURE 47

SASOL WAX MYU DATA: EFFECT OF CONVERSION
ON LCCO YIELD
WITH LOW ZEOLITE CONTENT CATALYSTS

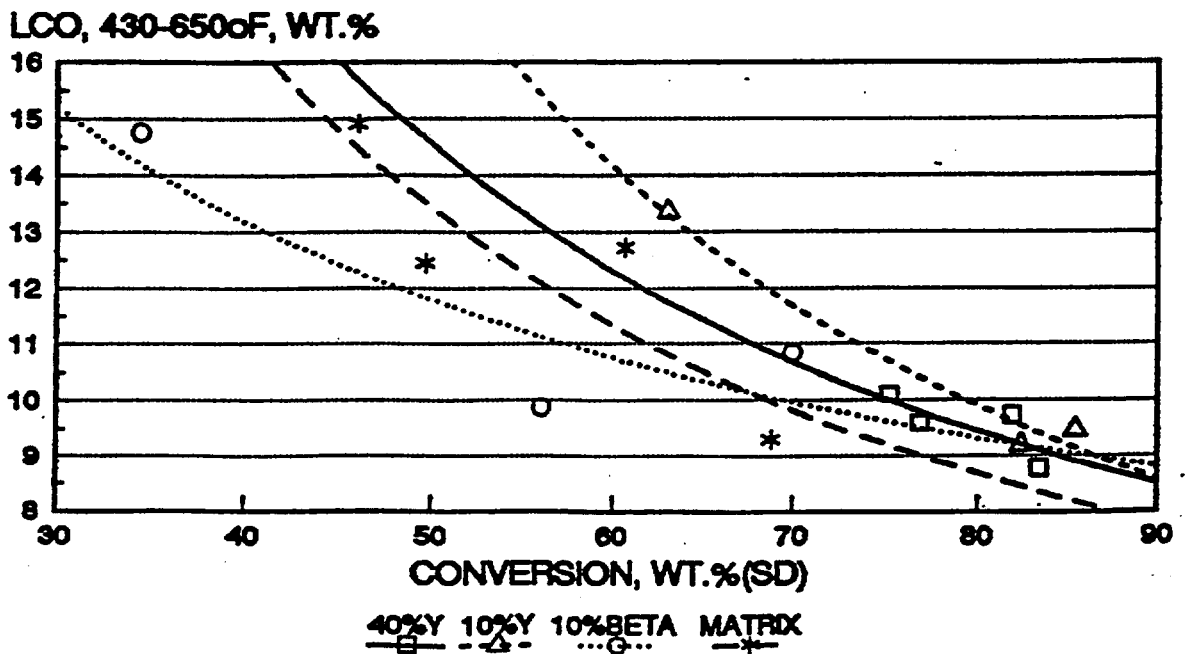


FIGURE 48

SASOL WAX MYU DATA: EFFECT OF CONVERSION
ON 650-800f CYCLE OIL YIELD
WITH LOW ZEOLITE CONTENT CATALYSTS

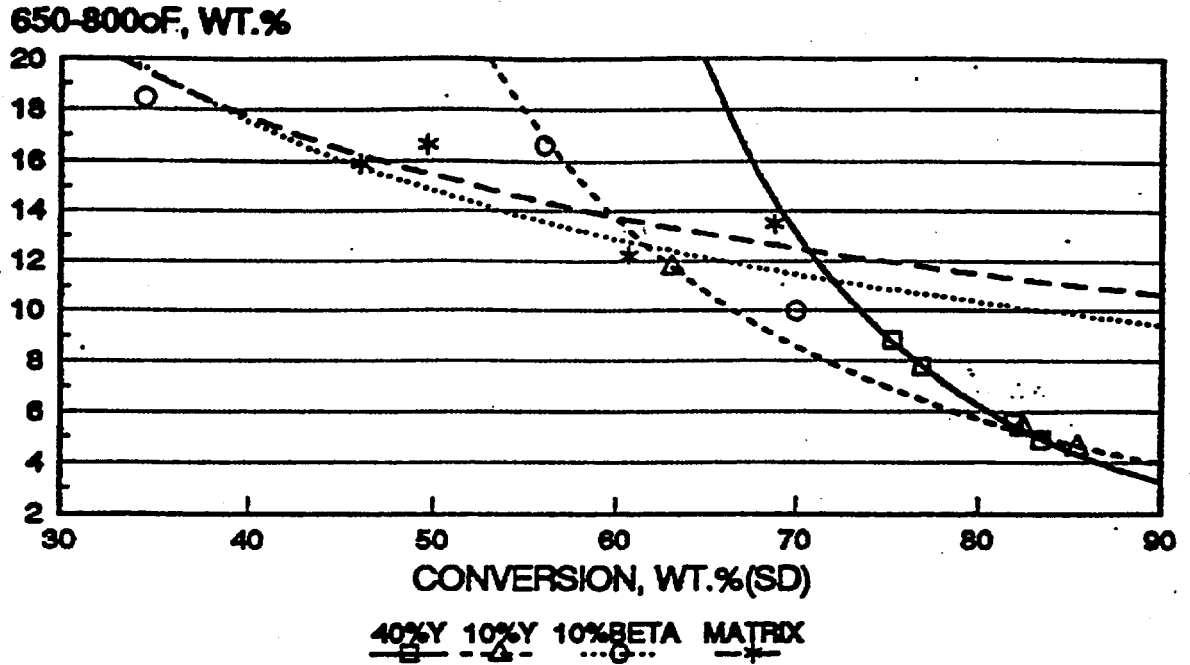


FIGURE 49

SASOL WAX MYU DATA: EFFECT OF CONVERSION
ON 800+F CYCLE OIL YIELD
WITH LOW ZEOLITE CONTENT CATALYSTS

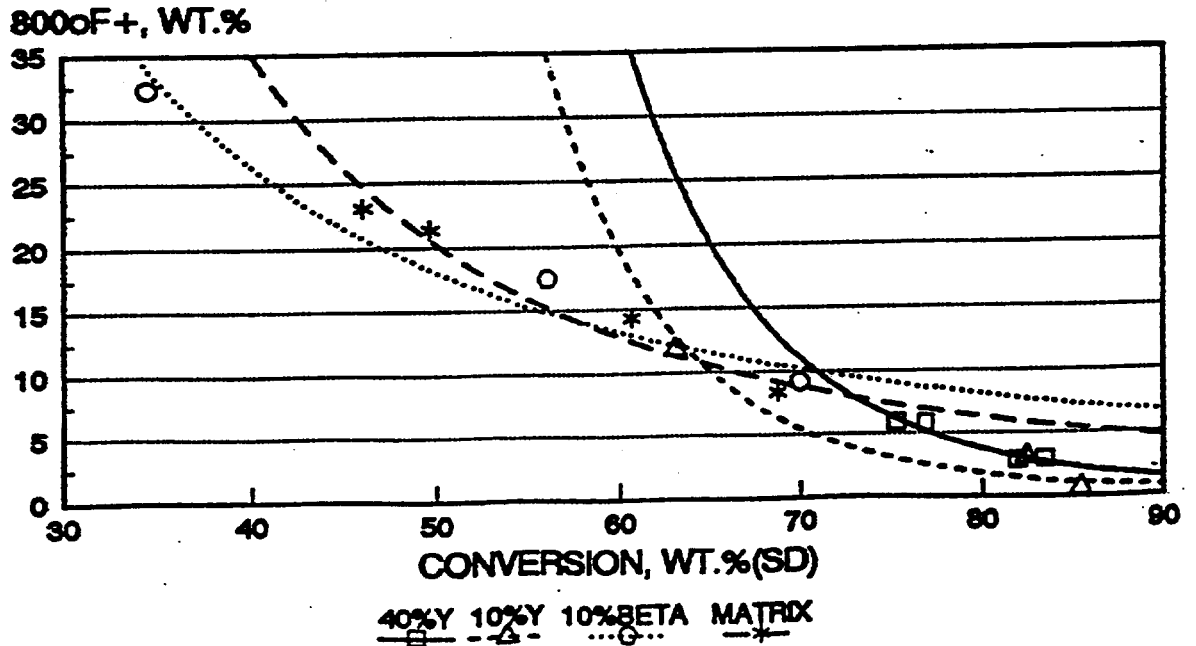


TABLE XIII

PHYSICAL PROPERTIES OF ZEOLITE FCC CATALYSTS
 Steam Treatment: 1450°F, 5 hours, 100% steam

Catalyst ID	Description	BET Surface Area, m ² /g			Micropore Volume (cc/g)
		Total	Zeolite	Matrix	
14059-81-4	40% Beta	211	143	68	.066
14040-48-1	40% Y	253	183	70	.084
14040-48-2	40% Y	233	167	66	.077
14040-50-5	Matrix	55	3.0	52	.001
14040-50-6	10% Y	90	48	42	.022
14040-50-7	10% Beta	69	19	50	.009

This would be done with high velocity air jets in the regenerator of a commercial FCC unit. The fines would then be removed from the flue gas by conventional electrostatic precipitators or other collection devices. A series of laboratory experiments, which are described below, demonstrated the feasibility of the selective attrition concept. Further effort would have been required to optimize the selective attrition process, and no additional work was made to test this processing option under the present contract. The catalytic cracking properties of this LaPorte wax feedstock were measured and compared with those of the Sasol wax after it was determined that the FCC process could tolerate the high level of iron catalyst fines in the LaPorte wax.

4.2.1 Selective Attrition Experiments

F-T fines-contaminated FCC catalyst to be used in selective attrition experiments was prepared by performing ten individual cracking runs with the same commercial equilibrium USY FCC catalyst using LaPorte wax feedstock. The runs were made at 970°F and 5 catalyst to oil ratio. This wax cracking sequence resulted in a significant deposition of F-T catalyst fines from the wax onto the FCC catalyst. Table XIV, Part A shows that the iron content of the FCC catalyst increased from 0.42% to 1.05%. This F-T fines-contaminated catalyst was the feed for a laboratory attrition test. A high velocity air jet subjected this catalyst sample to severe attrition conditions. After the attrition test, the catalyst and fines were recovered and analyzed for contaminant metals.

Table XIV, Part B, No. 2 shows that the F-T catalyst fines were selectively attritted from the contaminated FCC catalyst into the fines. The iron content of the contaminated FCC catalyst decreased from 1.05% to 0.62% after the attrition experiment. The selective attrition technique, although technically feasible, would not be economically viable because a commercial F-T wax would not contain the high level of iron that was present in the LaPorte wax used in these experiments. The iron content of the fines generated in this experiment was nearly 3%. Table XIV, Part B, No. 1 shows the results of a control attrition experiment that used the base catalyst without F-T catalyst fines. The composition of the fines, especially the iron content, was similar to the starting catalyst, which

TABLE XIV
MYU TESTS: SELECTIVE ATTRITION EXPERIMENTS

	(ppm)				
	Si	K	Fe	Cu	Al
A. F-T catalyst fines deposition, chemical analyses of samples (from LaPorte wax):					
1. Base catalyst CCC-1397	226000	121	4200	26	258000
2. Treated catalyst: 5.0 catalyst, 10 g LaPorte wax in 1 g segments ID No. 9363005 (15586-030-2P)	225000	266	10500	610	231000
B. Selective attrition experiments:					
1. Control:					
a. Starting sample CCC-1397	226000	121	4200	26	258000
b. After attrition (15586-030-1B)	200000	108	4200	21	254000
c. Fines (15586-030-1F)	252000	204	4100	14	235000
2. F-T catalyst contaminator sample 9363005:					
a. Starting sample (15586-030-2F)	225000	266	10500	610	231000
b. After attrition (15586-030-2B)	212000	159	6200	289	267000
c. Fines (15586-030-2F)	219000	125	29600	2020	213000

suggests that no selective attrition occurred with the uncontaminated, control sample.

A brief scanning electron microscopy (SEM) study of the catalyst and fines samples from these selective attrition experiments supported the conclusions of the chemical analyses. The series of SEM photographs shown in Figures 50-53 illustrates the fate of the FCC catalyst in these laboratory tests. Figure 50 shows that the base FCC catalyst consisted of varied shaped microspheres with smooth, rounded surfaces, a morphology that is characteristic of the abrasive nature of the circulating catalyst inventory of a commercial FCC unit. Figures 51 and 52 show the composition of the FCC catalyst after the sequential wax cracking experiments. These figures show that the F-T catalyst fines - which are small bright spots, due to the high iron content - were deposited mainly on the external surfaces of the FCC catalyst microspheres. Figure 53 shows the FCC catalyst sample after the selective attrition experiment. Most of the external F-T catalyst fines were removed from the external surfaces of the FCC catalyst. Figures 54 and 55 show that the fines from the attrition experiment consisted largely of very small, high iron content fragments.

4.2.2 Catalyst Effects

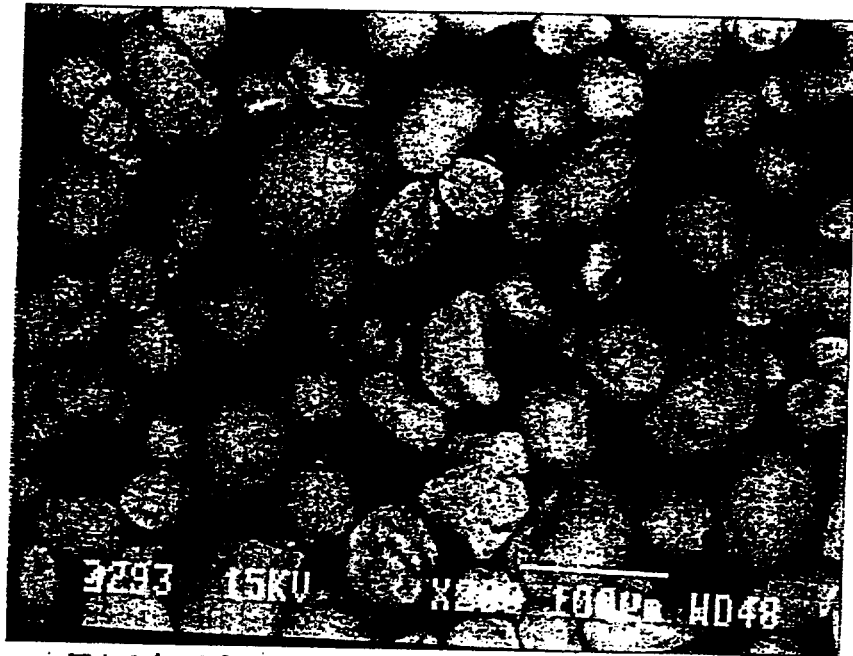
Catalytic cracking tests of the LaPorte wax feedstock were made with USY, HZSM-5, and beta zeolite catalysts. Table XV presents the detailed results of the catalytic cracking tests with the LaPorte wax and new test runs with the Sasol wax. The type of FCC catalyst, but not feedstock, had a major impact upon product yields and quality. Both feedstocks gave similar conversions and yields of the major catalytic cracking products. However, the presence of the iron F-T fines in the LaPorte wax increased the coke and hydrogen gas yields. In addition, small increases occurred in the octane quality of the naphtha products from the LaPorte wax feedstock.

This series of MYU tests nominally used the same reaction temperature of 970°F. The scatter of conversion values for both feedstocks and catalyst combinations between 80-90% at catalyst to oil ratios of 0.9-1.0, shown in Figure 56, suggests that both feedstocks had similar conversion values. Further tests at a wider variety of catalyst to oil ratios would be required to verify this tentative conclusion.

Figures 57 to 66 present product yields versus conversion plots for the wax feedstock and catalyst combinations. Figures 57 and 58 show that the coke and hydrogen gas yields, respectively, were significantly higher for the LaPorte wax than the Sasol wax. The iron F-T catalyst fines in the LaPorte wax were responsible for the higher coke and dehydrogenation because the same result was obtained using Sasol wax feedstock with USY catalyst that had 1% iron Fischer-Tropsch catalyst fines deposited upon its surface (Table XIV, Run No. 21; from the selective attrition experiments). The HZSM-5 catalyst, CCC-1891, had a lower coke yield but similar hydrogen yield compared with the other two catalysts for the LaPorte wax tests. The intermediate pore structure of the HZSM-5 catalyst apparently inhibited coke formation even in the presence of the active dehydrogenation catalyst, iron F-T fines. Figures 59-65, respectively, show propylene, isobutylene, isoamylenes, gasoline, distillate, 650-800°F cycle oil, and 800+°F cycle oil selectivity plots for the two wax feedstocks and the three catalysts. The major differences in product

FIGURE 50

SEM PHOTOGRAPH
BASE CATALYST = CCC-1397
EQUILIBRIUM FCC CATALYST
IRON CONTENT = 4200 PPM



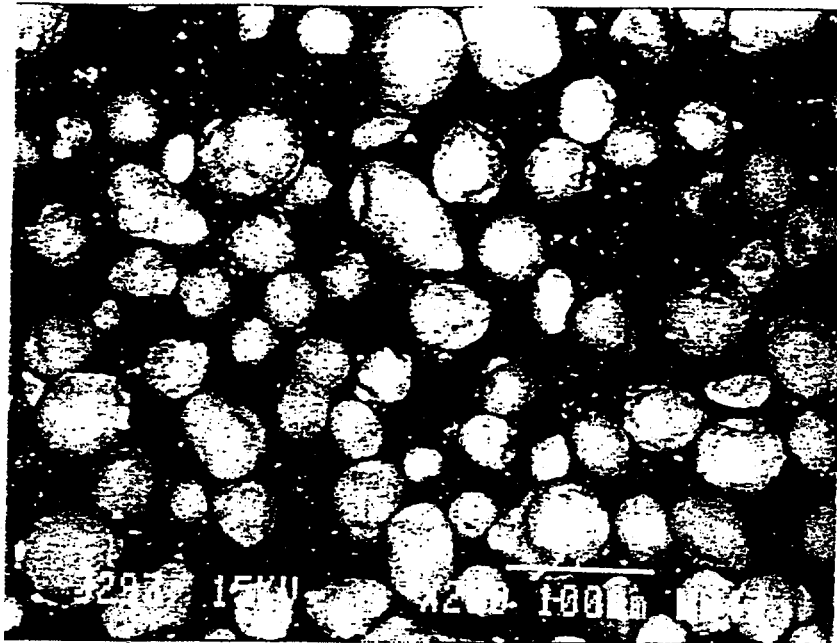
5586-230-1P BSE

FIGURES 51, 52

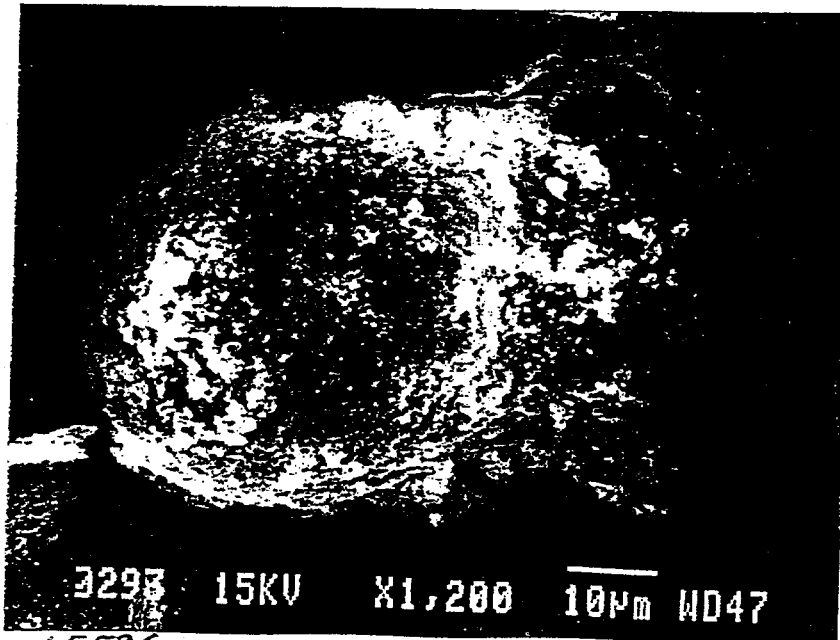
SEM PHOTOGRAPHS
F-T CATALYST FINES CONTAMINATED FCC CATALYST
BEFORE SELECTIVE ATTRITION EXPERIMENT

ID NO. 15586-030-2P

IRON CONTENT = 10500 PPM



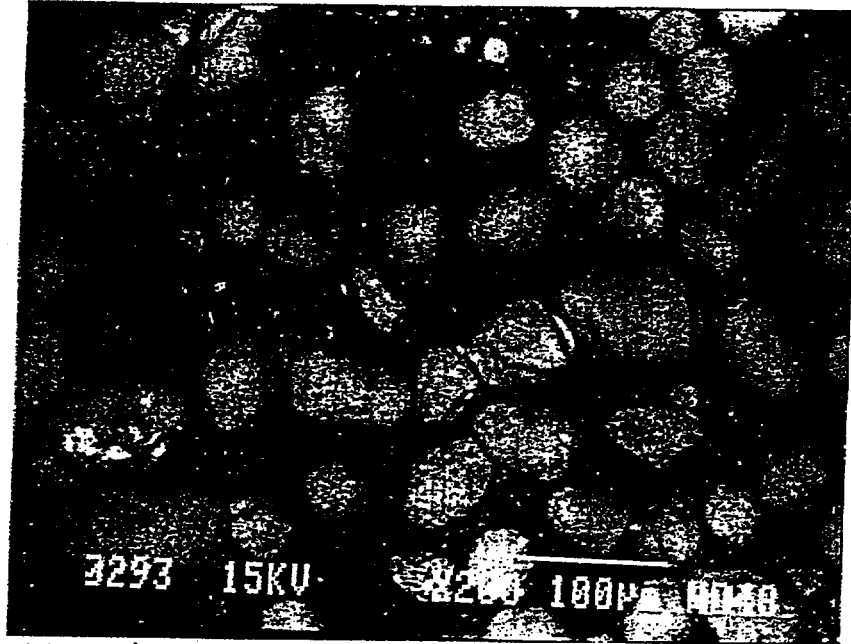
15586-030-20 ESE



15586-030-20 A-1

FIGURE 53

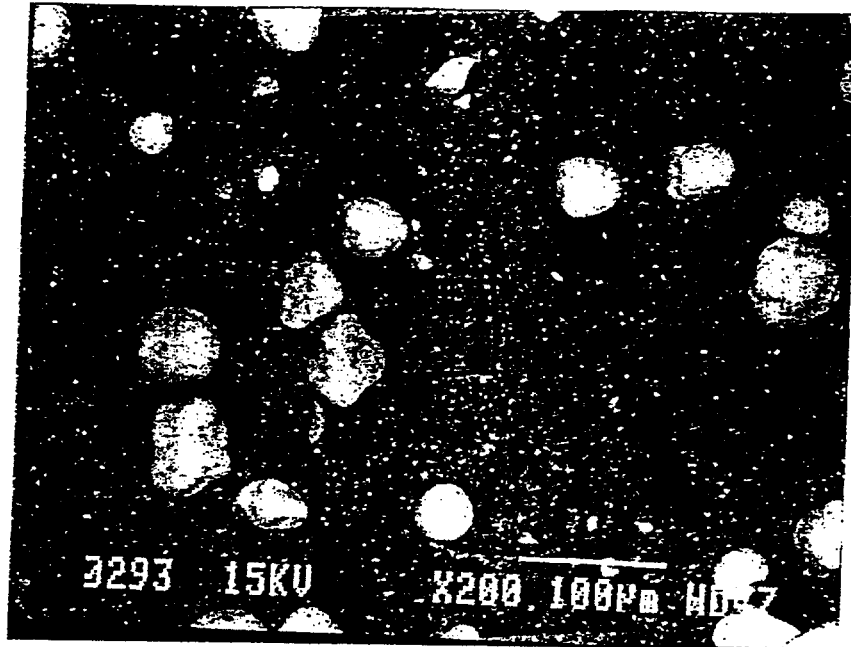
SEM PHOTOGRAPHS
F-T CATALYST FINES CONTAMINATED FCC CATALYST
AFTER SELECTIVE ATTRITION EXPERIMENT
ID NO. 15586-030-2B
IRON CONTENT = 6200 PPM



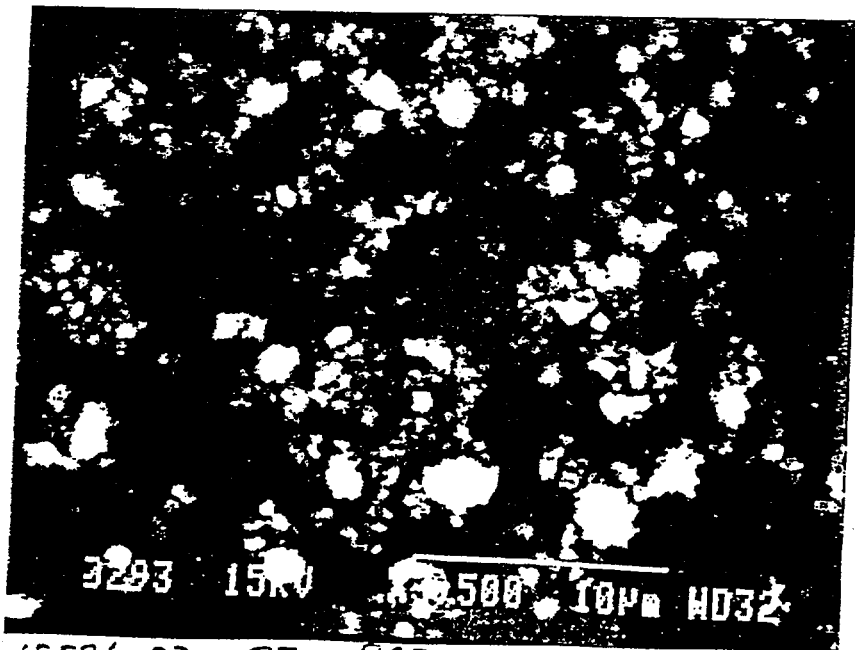
15586-030-2B BSE

FIGURES 54, 55

SEM PHOTOGRAPHS
CATALYST FROM SELECTIVE ATTRITION EXPERIMENT
ID NO. 15586-030-2F
IRON CONTENT = 29600 PPM



15586-030-2F BSE



15586-030-2F BSE A-1

FIGURE 56

LAPORTE VS SASOL WAX MYU DATA:
EFFECT OF C/O ON CONVERSION

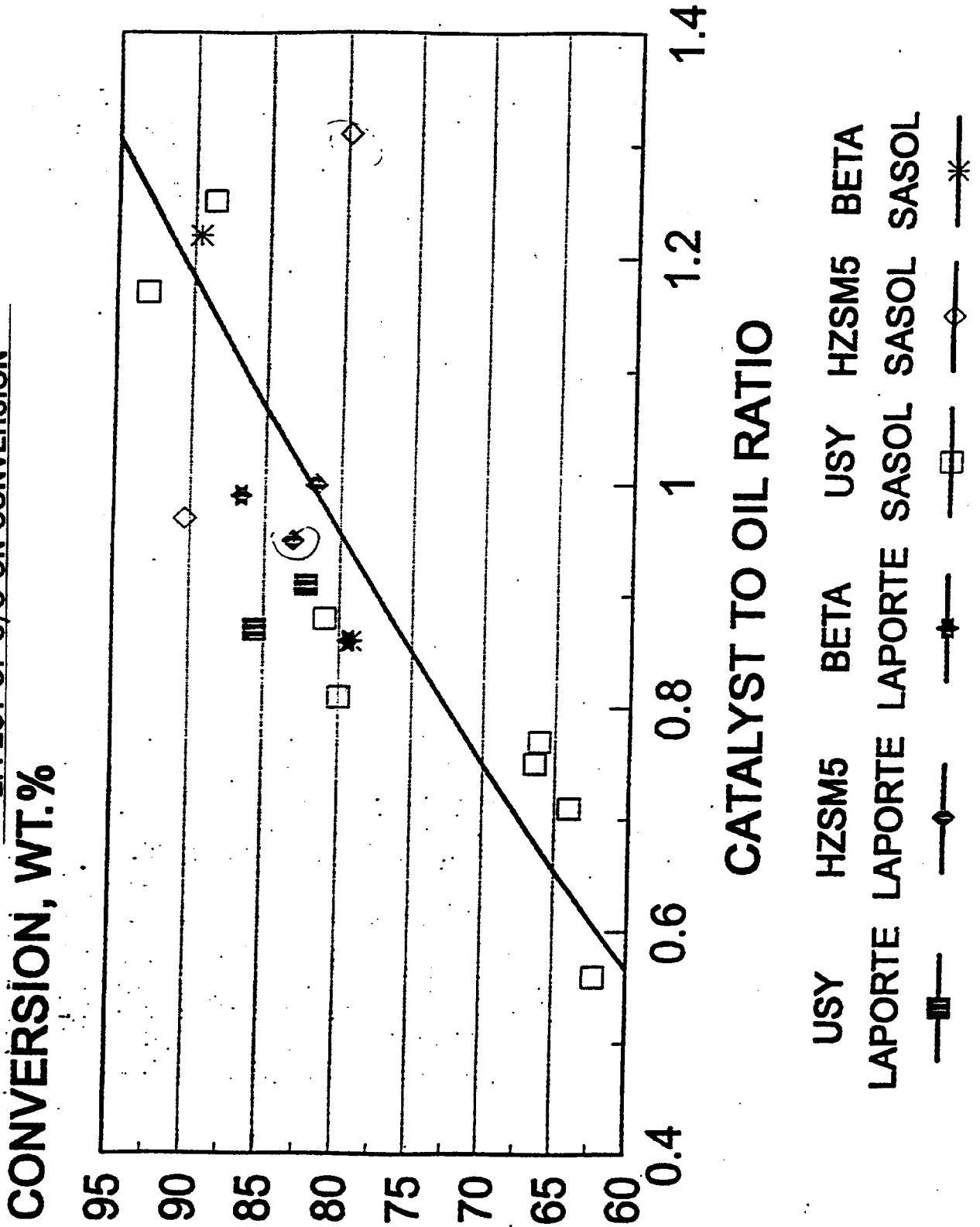


FIGURE 57

LAPORTE VS SASOL WAX MYU DATA:
EFFECT OF CONVERSION ON COKE

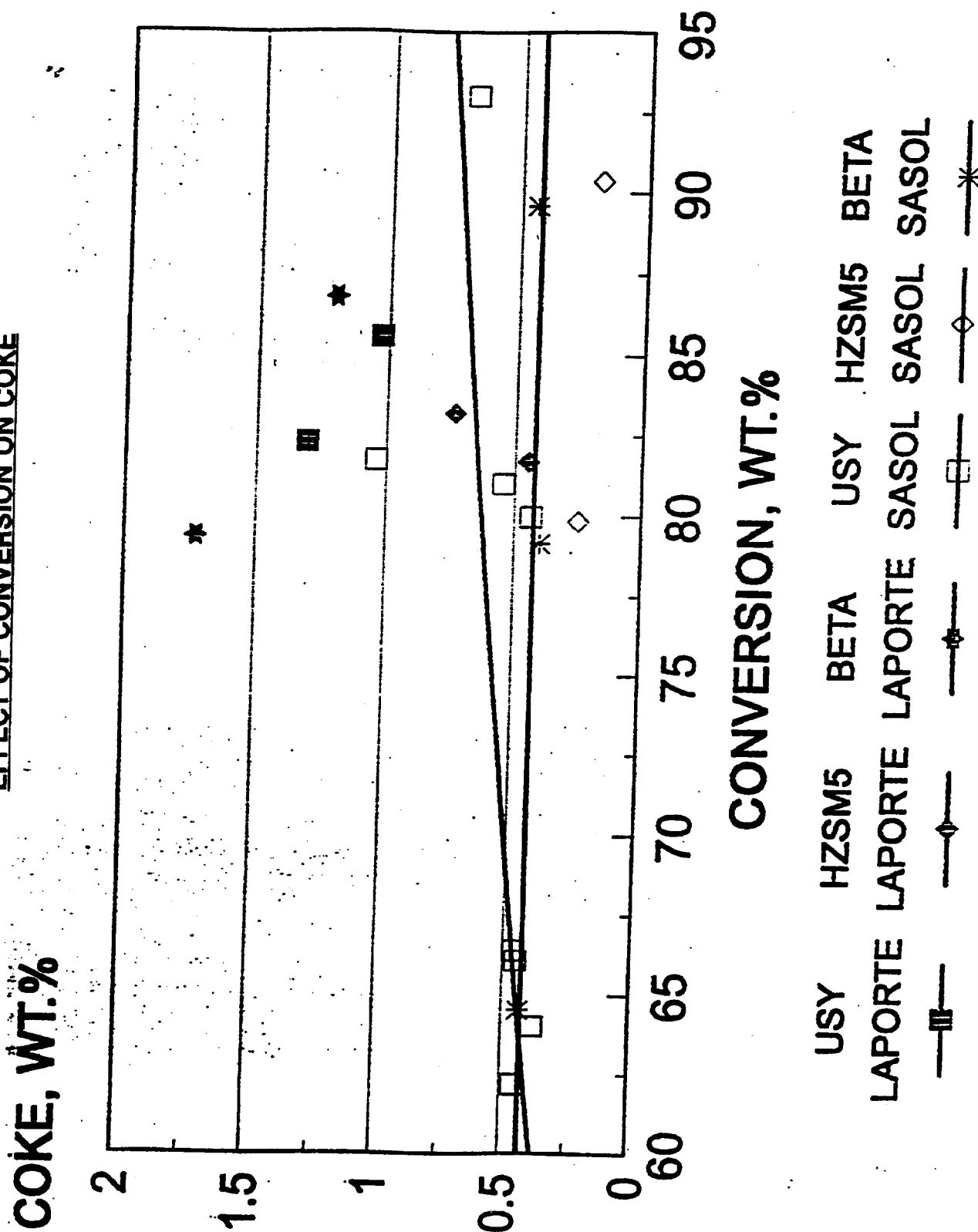


FIGURE 58

LAPORTE VS SASOL WAX MYU DATA:
EFFECT OF CONVERSION ON HYDROGEN YIELD

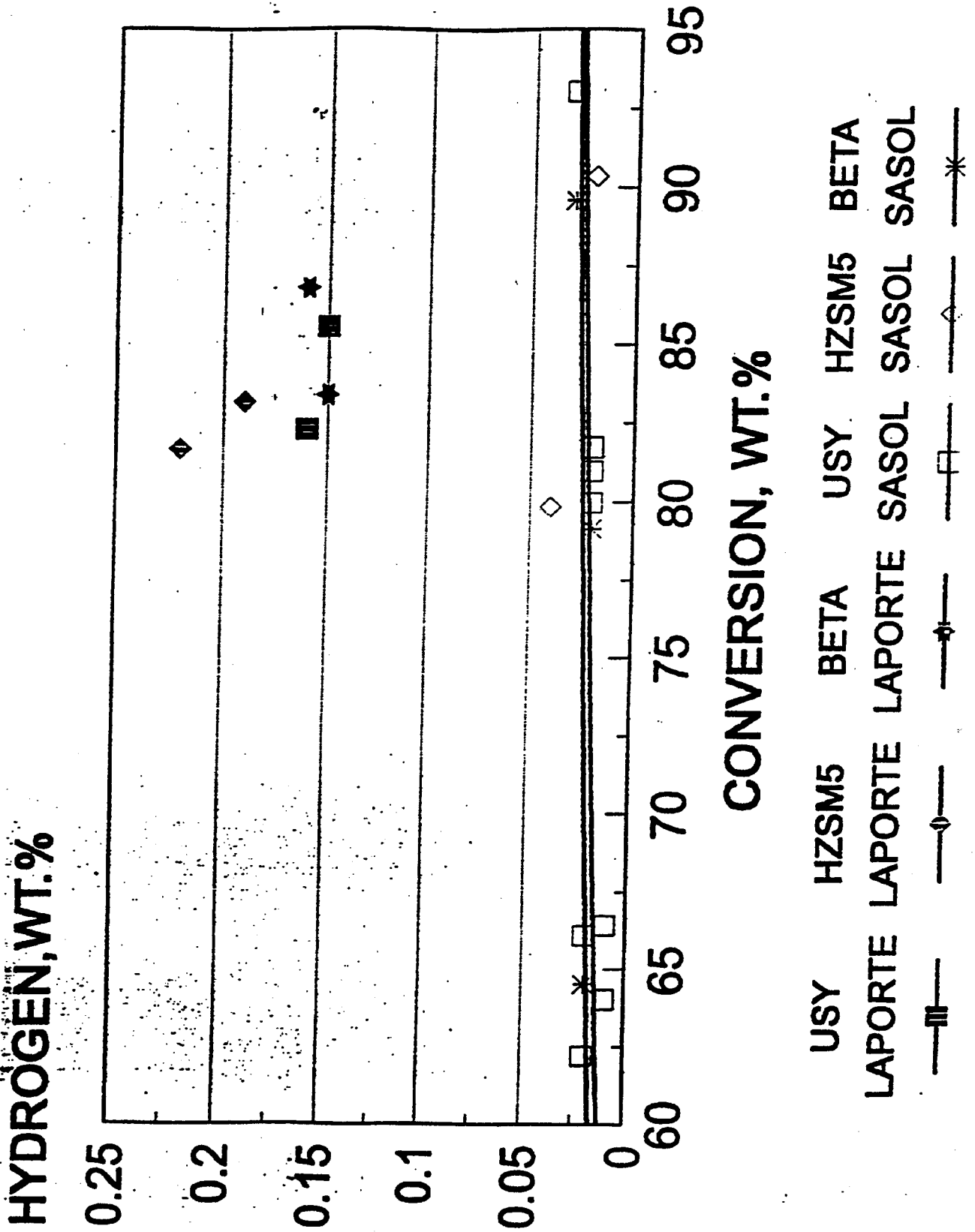


FIGURE 59

LAPORTE VS SASOL WAX MYU DATA:
EFFECT OF CONVERSION ON PROPYLENE YIELD

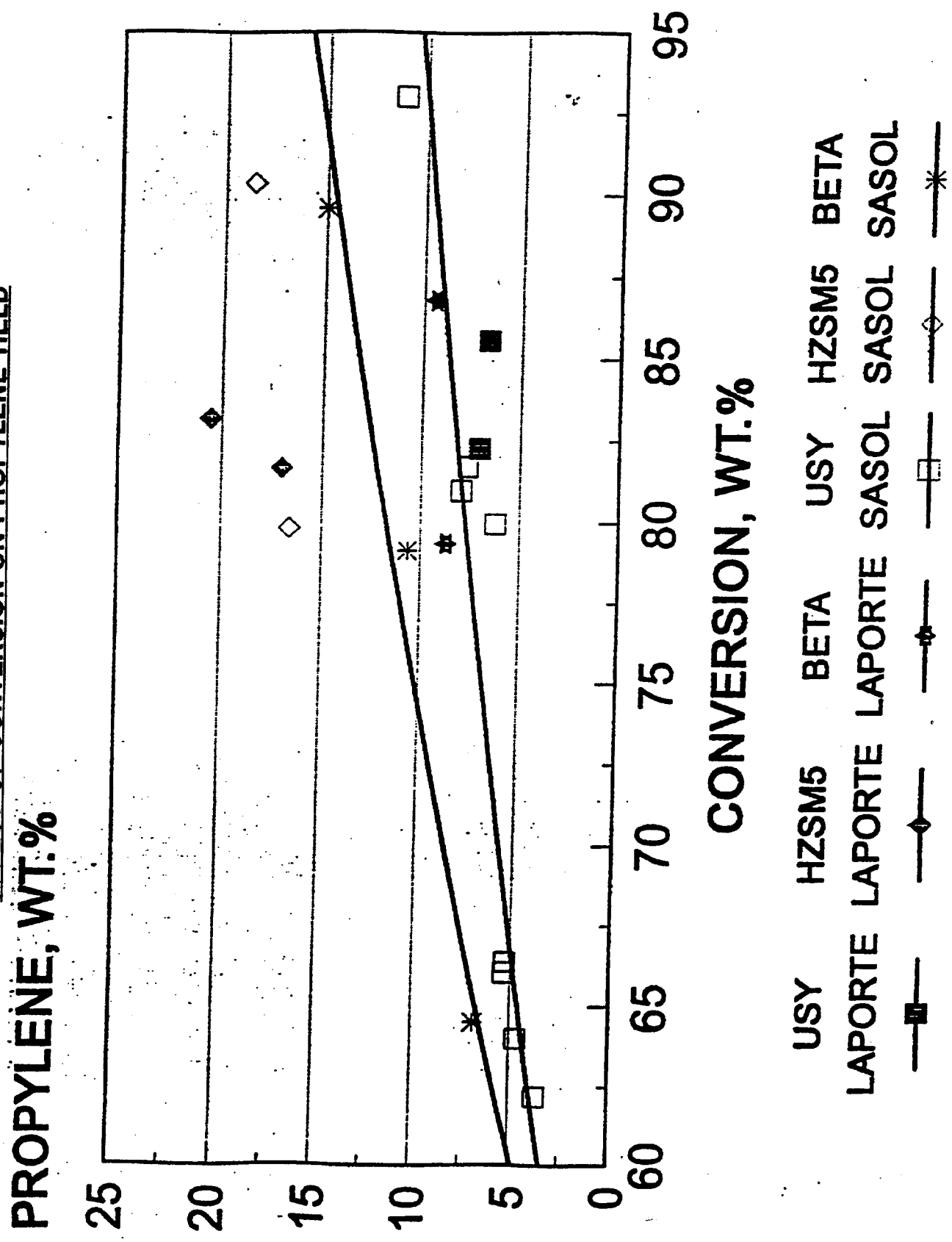


FIGURE 60

LAPORTE VS SASOL WAX MYU DATA:
EFFECT OF CONVERSION ON ISOBUTYLENE YIELD

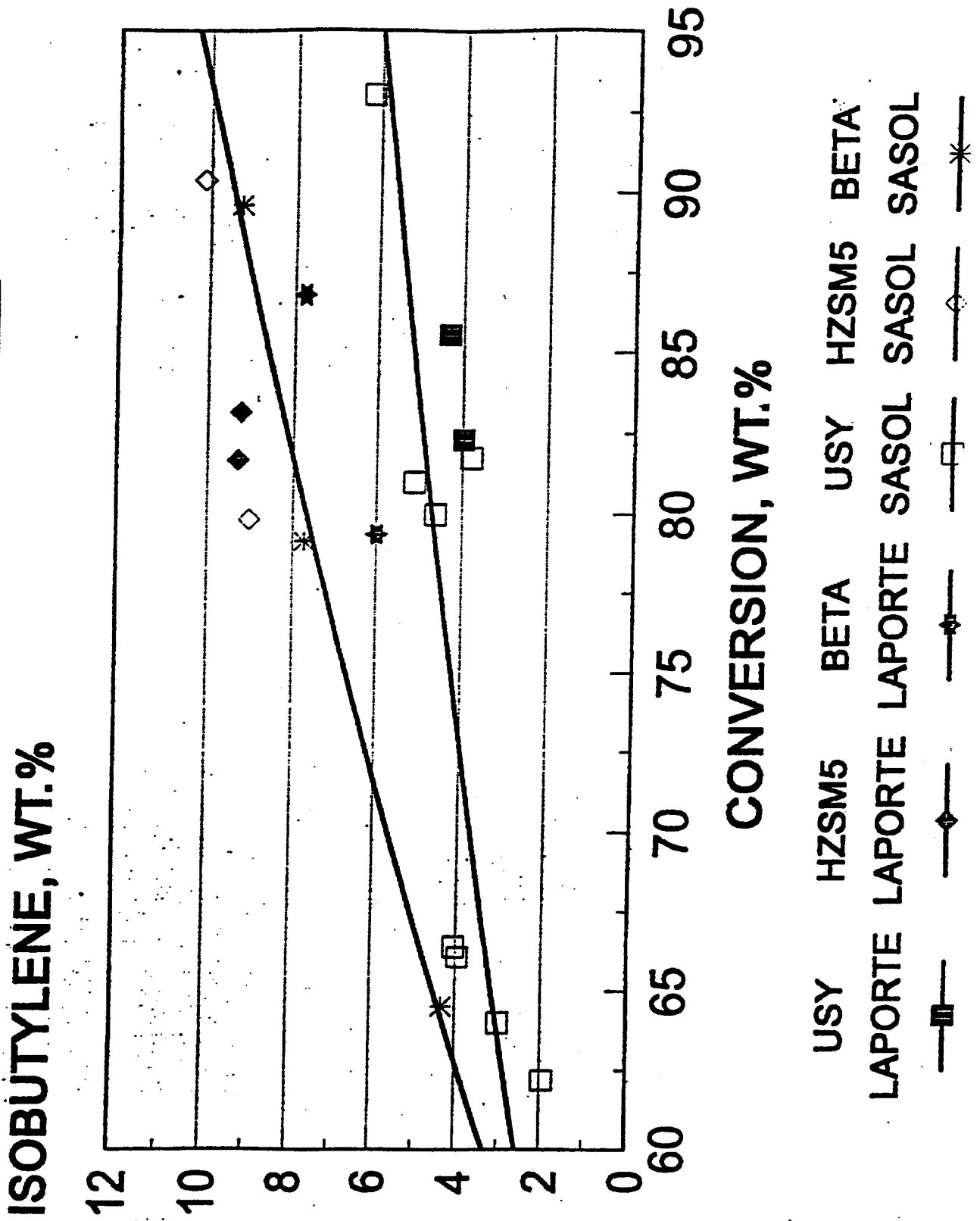


FIGURE 61
LAPORTE VS SASOL WAX MYU DATA:
EFFECT OF CONVERSION ON ISOAMYLENES YIELD

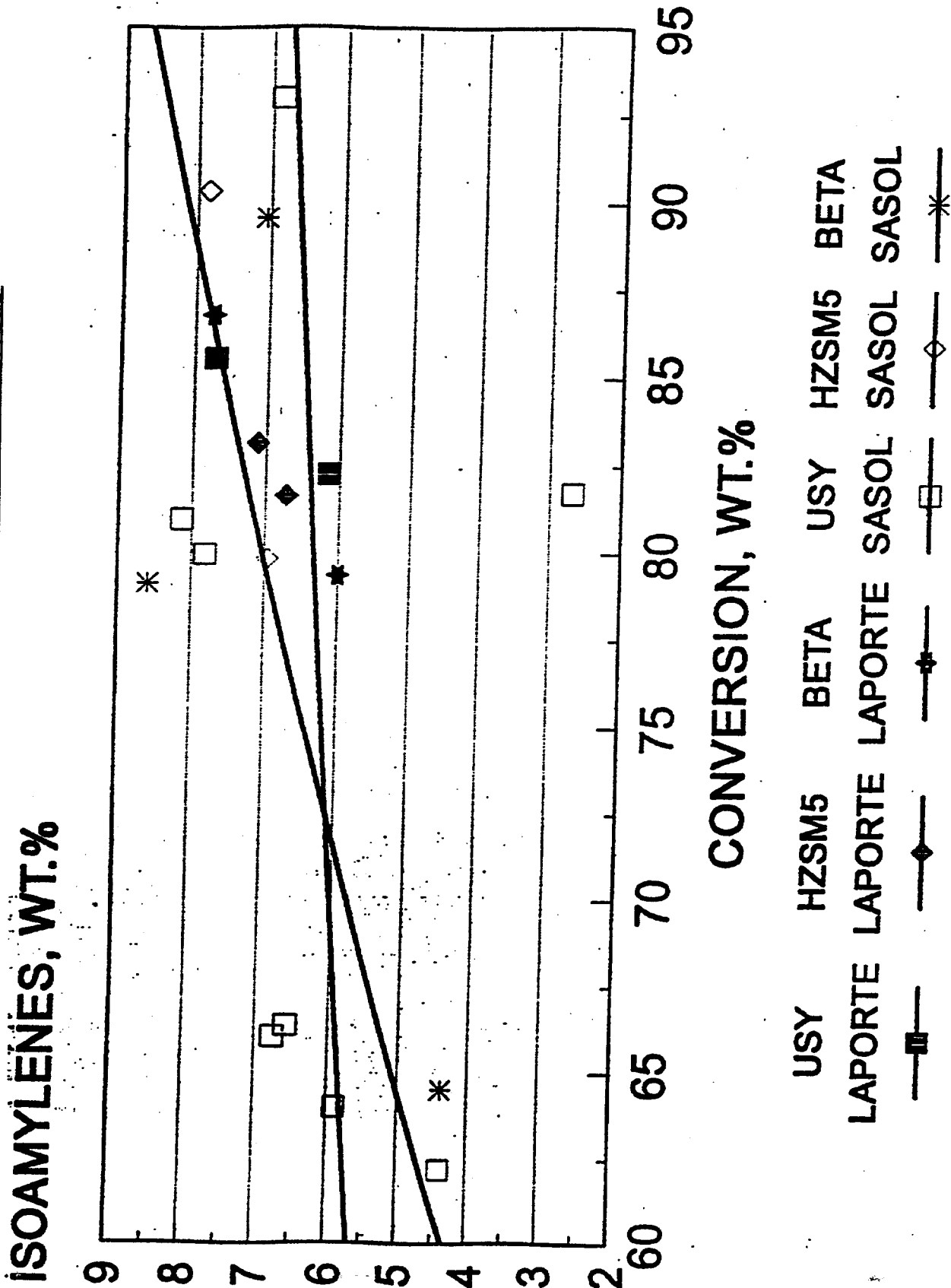
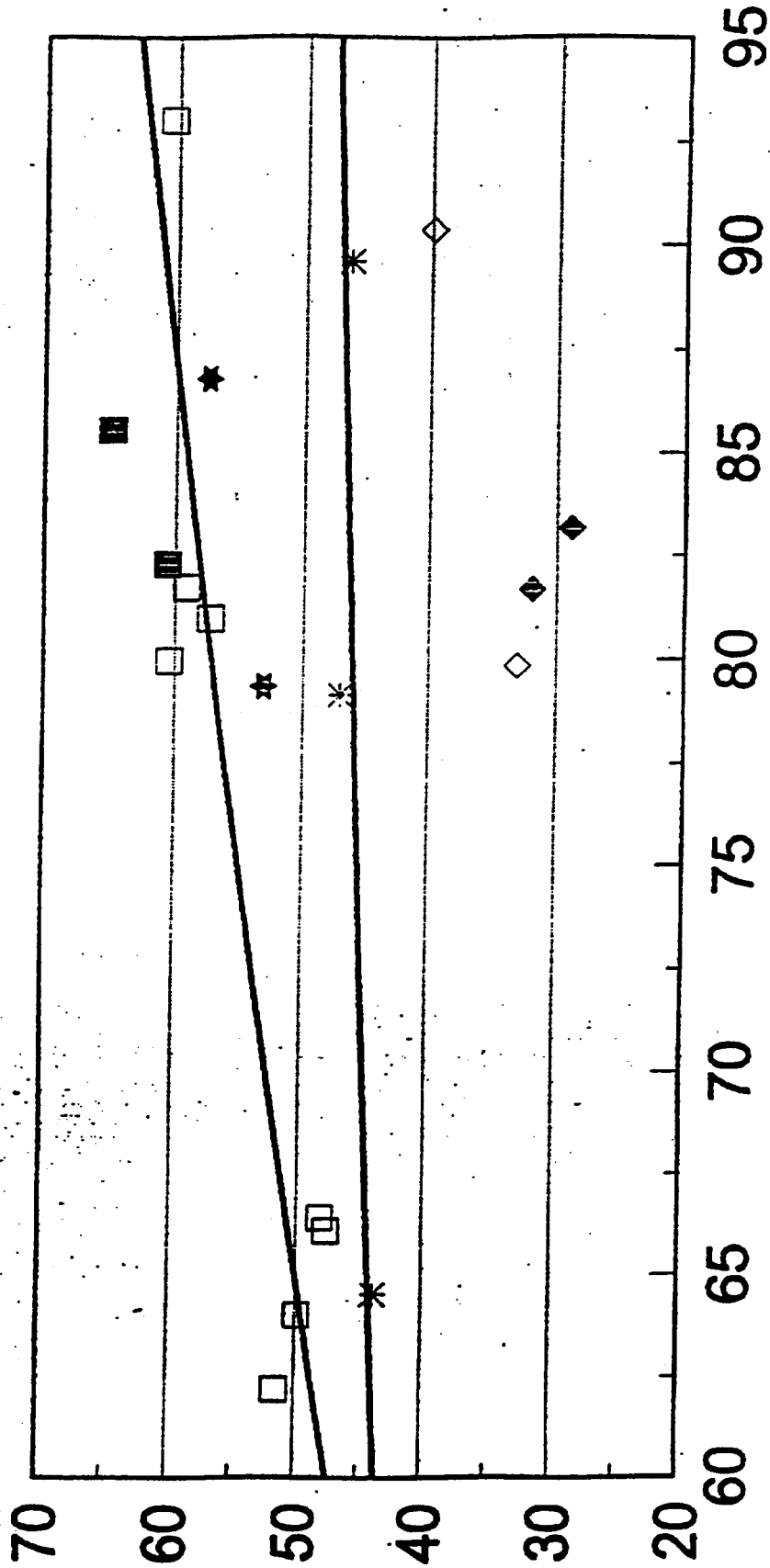


FIGURE 62

LAPORTE VS SASOL WAX MYU DATA:
EFFECT OF CONVERSION ON C5-430F NAPHTHA YIELD

C5-430oF, NAPHTHA, WT.%



CONVERSION, WT.%

USY HZSM5 BETA USY HZSM5 BETA
LAPORTE LAPORTE SASOL SASOL SASOL

FIGURE 63

LAPORTE VS SASOL WAX MYU DATA:
EFFECT OF CONVERSION ON LCCO YIELD

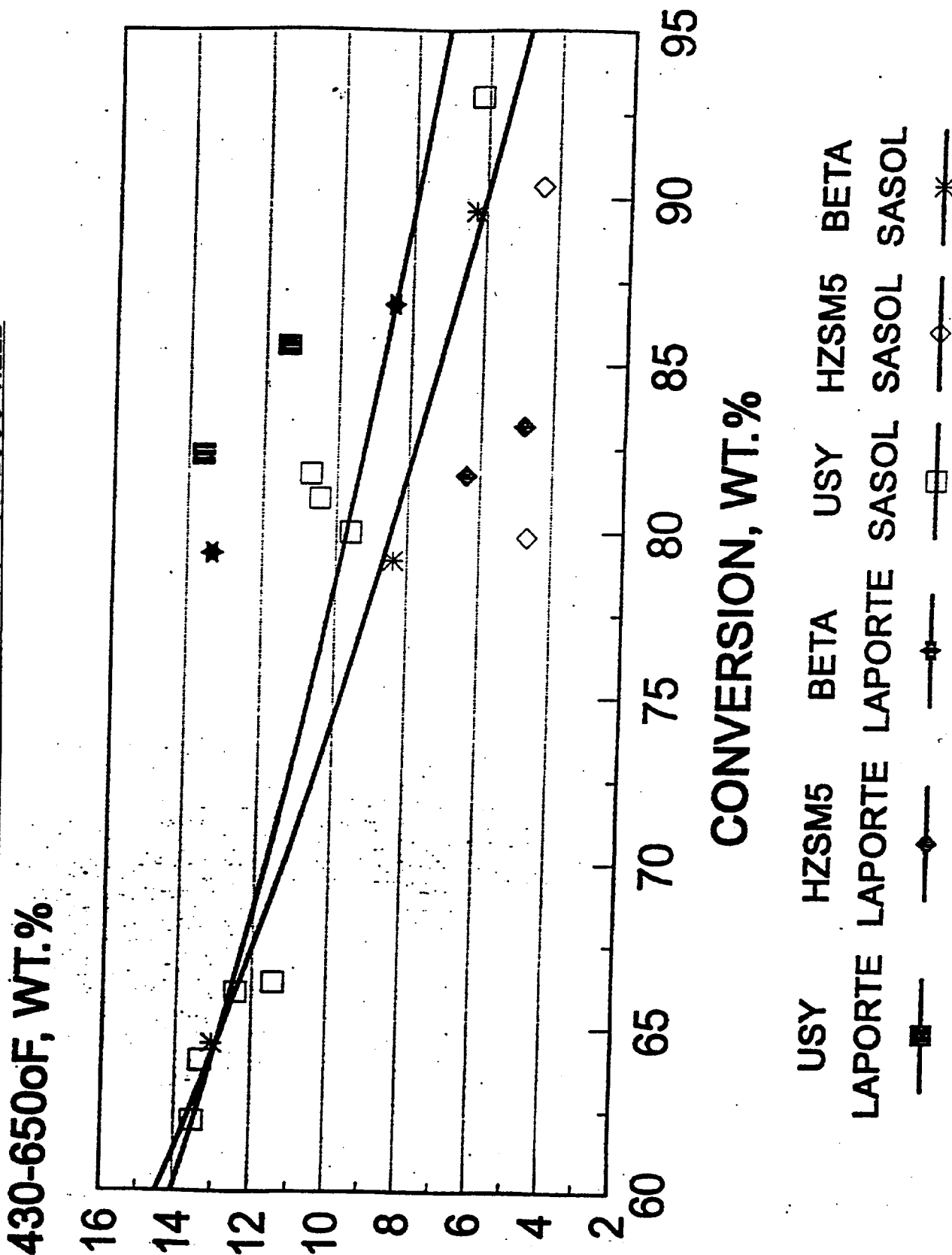
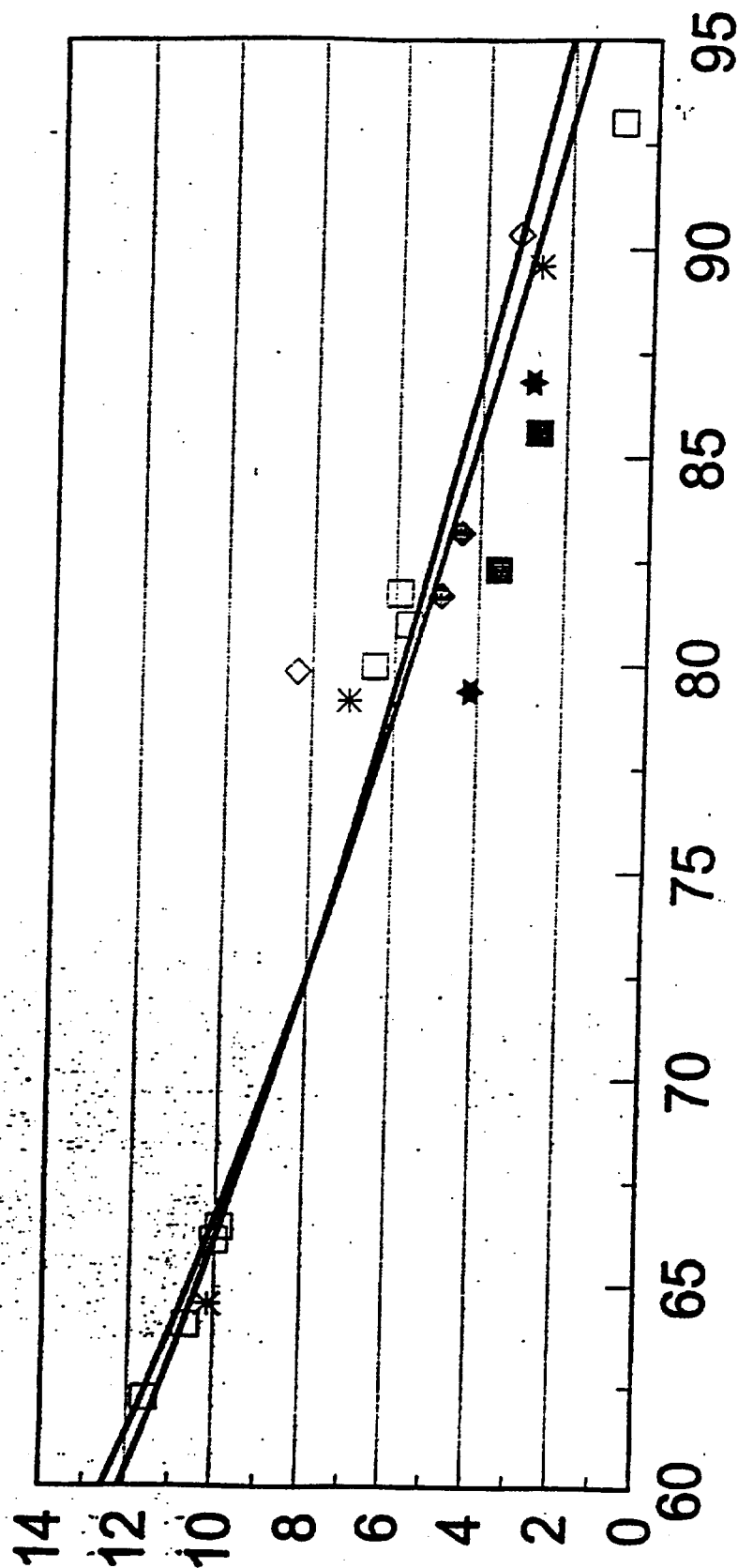


FIGURE 64

LAPORTE VS SASOL WAX MYU DATA:
EFFECT OF CONVERSION ON 650-800°F CYCLE OIL YIELDS

650-800°F, WT.%



CONVERSION, WT.%

USY HZSM5 BETA USY HZSM5 BETA
LAPORTE LAPORTE SASOL SASOL SASOL SASOL

—■— —◆— —*— —◆— —*—

FIGURE 65
BOTTOMS SELECTIVITY SASOL AND LAPORTE WAX

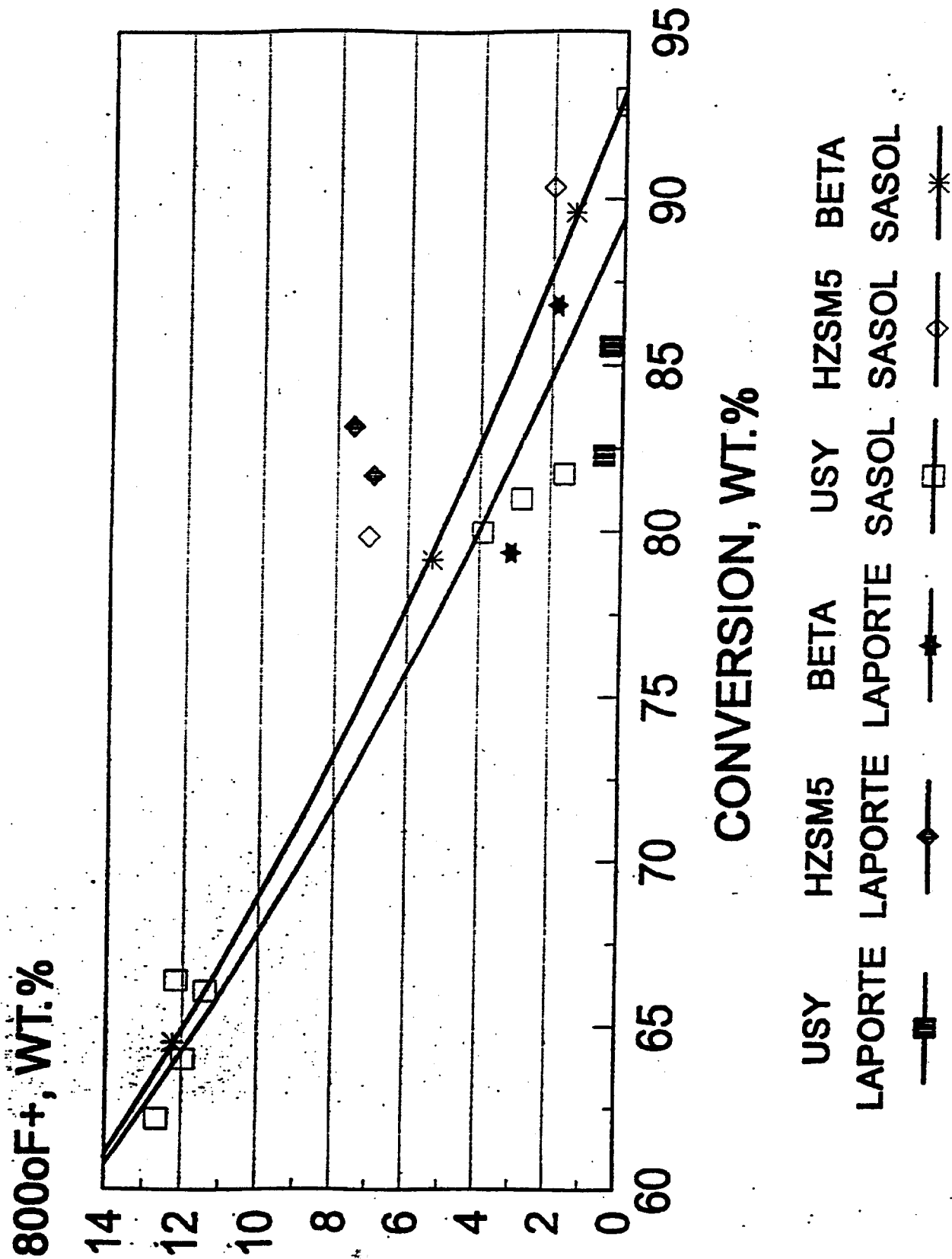


FIGURE 66

LAPORTE VS SASOL WAX MYU DATA:
EFFECT OF CONVERSION ON RON

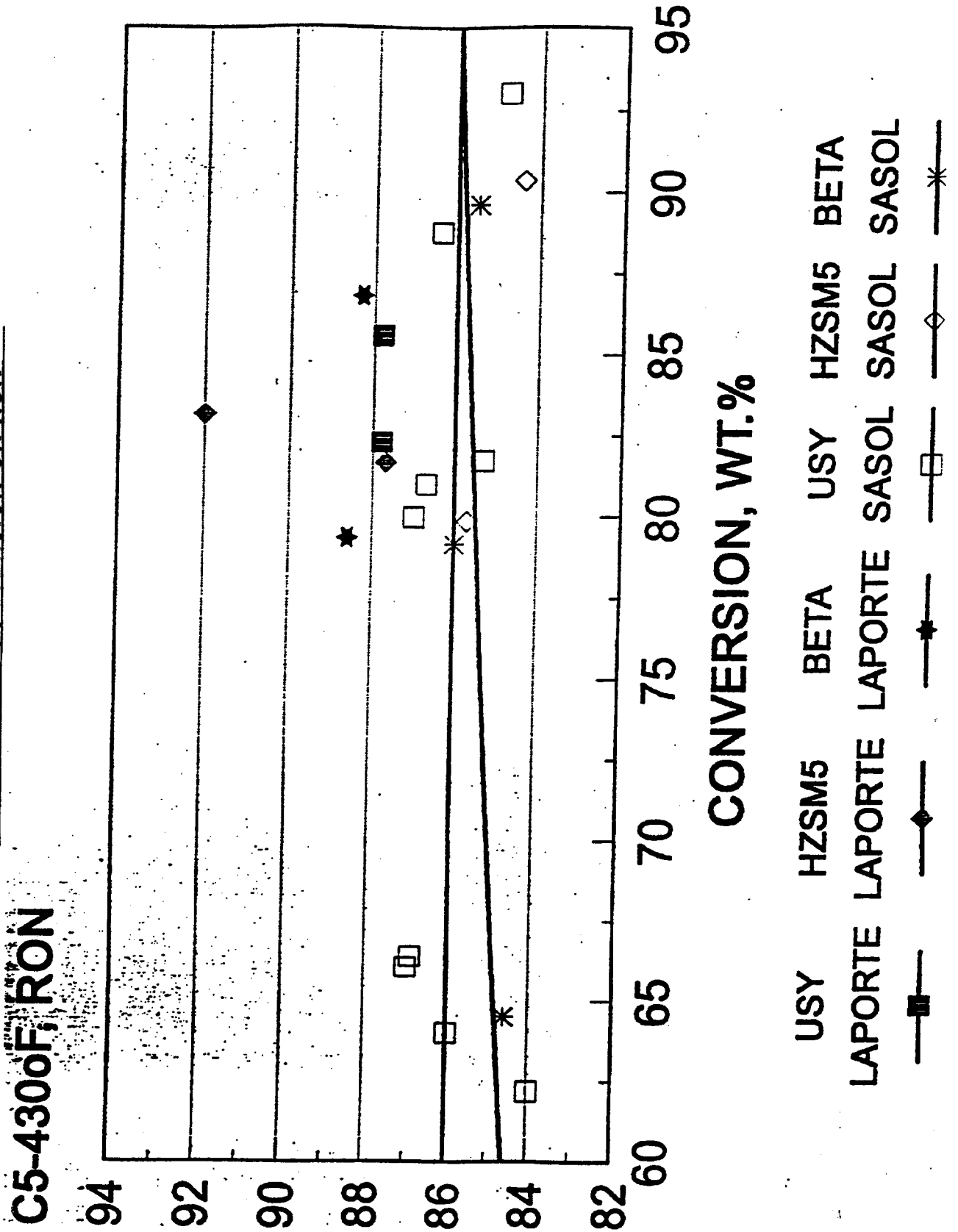


TABLE XV

MYU TESTS: SASOL VS LAPORTE WAX FEEDSTOCKS
(Catalytic Cracking, 970F, 0.8 Catalyst/Oil)
(Continued)

Feed: Sasol Wax		Weight Percent Product Yields										C ₅ -430°F					Gasoline Composition, Wt% on Feed				
Catalyst	Run #	Conv. Wt%	H ₂	C ₃	1C ₄	1C ₅	C ₆ -430°F	Coke	430-650°F	650-800°F	800°F+	RON	MON	P ₁₀₀	I ₁₀₀	A ₁₀₀	N ₁₀₀	O ₁₀₀			
9363005*	A 021	86.2	0.16	9.89	4.16	4.57	53.11	2.60	--	--	--	86.4	78.7	--	--	--	--	--			
	B 021	88.73	--	10.07	4.24	4.20	54.96	2.61	9.23	1.64	.397	--	--	--	--	--	--	--			
	A 022	75.7	0.02	9.03	4.43	3.49	49.38	0.95	--	--	--	85.3	76.5	6.93	20.48	25.52	12.37	31.76			
	B 022	81.74	--	7.66	3.79	2.68	59.13	1.04	10.73	5.91	1.61	--	--	--	--	--	--	--			
	A 023	56.4	0.02	3.79	1.88	2.08	45.15	0.45	--	--	--	84.0	74.5	5.77	19.09	18.17	15.15	35.58			
	B 023	62.2	--	3.68	1.95	4.40	51.54	.45	13.53	11.60	12.65	--	--	--	--	--	--	--			
GCC 1891 (HZSM-5)	A 024	62.0	0.01	5.18	3.71	4.93	43.28	0.46	--	--	--	86.9	76.6	4.31	20.03	16.57	14.60	38.60			
	B 024	66.42	--	5.29	4.05	6.58	48.09	.46	11.46	9.91	12.19	--	--	--	--	--	--	--			
	A 025	67.2	0.02	5.20	3.69	5.41	48.52	0.44	--	--	--	87.0	76.5	4.59	19.37	15.87	14.0	40.07			
	B 025	66.1	--	5.33	3.96	6.76	47.61	0.45	12.44	10.03	11.42	--	--	--	--	--	--	--			
	A 026	78.2	0.02	6.34	4.42	6.70	56.5	0.43	--	--	--	87.0	76.4	5.03	20.41	12.86	11.43	43.9			
	B 026	79.99	--	6.22	4.63	7.82	60.41	.435	9.597	6.49	3.91	--	--	--	--	--	--	--			
GCC 1875 (Beta)	A 027	61.6	0.01	4.65	2.78	4.02	46.88	0.38	--	--	--	86.0	75.5	4.66	19.44	15.64	14.19	39.73			
	B 027	64.03	--	4.67	3.00	5.89	49.87	.38	13.34	10.67	11.97	--	--	--	--	--	--	--			
	A 009	87.7	--	18.64	10.13	7.64	36.94	0.19	--	--	--	84.4	75.5	15.5	6.88	11.81	8.48	46.84			
	B 009	90.35	--	18.56	10.13	7.85	39.87	.186	4.44	3.2	1.99	--	--	--	--	--	--	--			
	A 018	74.7	--	16.53	8.94	6.74	28.23	0.25	--	--	--	85.7	76.3	15.59	7.66	18.49	10.25	39.13			
	B 018	79.86	--	16.58	9.01	6.96	33.00	.25	4.67	8.36	7.10	--	--	--	--	--	--	--			
GCC 1875 (Beta)	A 010	90.9	--	14.89	9.15	7.91	47.32	0.42	--	--	--	85.5	76.5	10.38	12.85	15.21	9.87	41.31			
	B 010	89.6	--	14.96	9.26	7.06	46.41	.44	6.29	2.70	1.38	--	--	--	--	--	--	--			
	A 012	79.8	--	10.78	7.59	7.72	46.25	0.38	--	--	--	86.0	75.8	8.85	13.37	12.47	11.60	48.08			
	B 012	79.16	--	10.65	7.73	8.59	47.00	.40	8.39	7.11	5.33	--	--	--	--	--	--	--			
	A 019	57.2	--	6.74	4.19	3.95	37.04	0.42	--	--	--	84.6	75.8	7.98	14.68	19.34	15.85	33.16			
	B 019	64.53	--	6.88	4.33	4.39	43.81	.436	13.05	10.16	12.25	--	--	--	--	--	--	--			

*A - MYU Conversion Calculation

B - Simulated Distillation Conversion Calculation

**P - paraffin

I - isoparaffin

A - aromatic

N - naphthene

O - olefin

MMS/1kv/93411

7/26/93